FLS2 is a CDK-like kinase that directly binds IFT70 and is required for proper ciliary disassembly in *Chlamydomonas*

Qin Zhao[1], Shufen Li[1], Shangjin Shao[1], Zhengmao Wang[1] and Junmin Pan[1,2*]

[1]MOE Key Laboratory of Protein Sciences, Tsinghua-Peking Center for Life Sciences, School of Life Sciences, Tsinghua University, Beijing 100084, China

[2]Laboratory for Marine Biology and Biotechnology, Qingdao National Laboratory for Marine Science and Technology, Qingdao, Shandong Province 266000, China

Running title: A CDK-like kinase and cilia disassembly

***Correspondence:**

panjunmin@tsinghua.edu.cn; Tel/Fax 0086-1062771864

Abstract

Intraflagellar transport (IFT) is required for ciliary assembly and maintenance. While disruption of IFT may trigger ciliary disassembly, we show here that IFT mediated transport of a CDK-like kinase ensures proper ciliary disassembly. Mutations in flagellar shortening 2 (*FLS2*), encoding a CDK-like kinase, lead to retardation of cilia resorption and delay of cell cycle progression. Stimulation for ciliary disassembly induces gradual dephosphorylation of FLS2 accompanied with gradual inactivation. Loss of FLS2 or its kinase activity induces early onset of kinesin13 phosphorylation in cilia. FLS2 is predominantly localized in the cell body, however, it is transported to cilia upon induction of ciliary disassembly. FLS2 directly interacts with IFT70 and loss of this interaction inhibits its ciliary transport, leading to dysregulation of kinesin13 phosphorylation and retardation of ciliary disassembly. Thus, this work demonstrates that IFT plays active roles in controlling proper ciliary disassembly by transporting a protein kinase to cilia to regulate a microtubule depolymerizer.

Key words: Cilia and flagella; IFT; Ciliary disassembly; CDK-like kinase; *Chlamydomonas*

Author Summary

Cilia or eukaryotic flagella are cellular surface protrusions that function in cell motility as well as sensing. They are dynamic structures that undergo assembly and disassembly. Cilia are resorbed during cell cycle progression. Dysregulation of cilia resorption may cause delay of cell cycle progression, which underlies aberrant cell differentiation and even cancer. Ciliary resorption requires depolmerization of axonemal microtubules that is mediated by kinesin13. Using the unicellular green alga, *Chlamydomonas*, we have identified a CDK-like kinase FLS2 that when mutated retards cilia resorption, leading to delay of cell cycle progression. FLS2, a cell body protein, is transported to cilia via intraflagellar transport upon induction of cilia resorption. FLS2 directly interacts with IFT70 and loss of this interaction inhibits transport of FLS2 to cilia and fails to regulate proper phosphorylation of kinesin13 in cilia.

Introduction

Cilia are microtubule-based cellular structures that extend from the cell surface. The cellular motility and signaling mediated by cilia plays pivotal roles in physiology and development [1, 2]. The medical importance of cilia is underscored by at least 35 ciliopathies that are caused by mutations in around 200 cilia-related genes [3].

Cilia are dynamic structures that undergo assembly and disassembly. They are assembled after cell division and disassembled prior to and/or during mitosis [4-7]. They are also subjected to disassembly during cell differentiation and in response to cellular stress [8-10]. Ciliary disassembly may occur via deflagellation/deciliation (shedding of whole cilium or flagellum) or resorption (gradual shortening from the ciliary tip) depending on physiological context and/or stimulus [8, 11, 12]. During cell cycle progression in mammalian cells as well as in *Chlamydomonas*, cilia are resorbed [4, 5, 7, 13, 14]. However, deciliation has also been reported as a predominant mode of ciliary disassembly during cell cycle progression in mammalian cells [15]. Defect in ciliary resorption has been shown to inhibit G1-S transition and delays cell cycle progression [16-20], which leads to premature differentiation of neural progenitors [18, 20, 21]. Several studies also suggest that ciliary disassembly is related to tumorigenesis because primary cilia are disassembled in a variety of cancer types [22].

Cilia resorption is trigged by a series of signal cascades that almost all lead to activation of aurora-A [7, 10, 23]. Aurora-A further activates microtubule deacetylase HDAC6 and inhibition of which impairs ciliary disassembly [7]. Microtubule depolymerizing kinesins also function in ciliary resorption to mediate disassembly of axonemal microtubules. Depletion of microtubule depolymerases kinesin13s in *Chlamydomonas* (CrKinesin13) or mammalian cells (KIF2A and KIF24) inhibits ciliary disassembly [20, 24-26].

Intraflagellar transport (IFT) ferries ciliary proteins to build and maintain cilia [27, 28].

Conditional inactivation of IFT motor kinesin-2 induces ciliary disassembly in both mammalian cells and in *Chlamydomonas* [23, 29-31], suggesting that cells may employ the mechanism of inactivation of IFT machinery to trigger ciliary disassembly. However, it has been shown that IFT proteins are actually increased in resorbing cilia upon cilia resorption that occurs during zygote development or in response to extracellular stimuli in *Chlamydomonas* [32, 33], implying that IFT may be involved in ciliary resorption triggered by internal or external stimuli. Thus, further evidence is needed to pinpoint the role of IFT in ciliary resorption.

In this report, we have identified a CDK-like kinase, flagellar shortening 2 (FLS2) that functions in ciliary resorption in *Chlamydomonas*. FLS2 promotes ciliary shortening by a mechanism in which it is transported to cilia by directly binding IFT70 to control proper phosphorylation of kinesin13 in cilia.

Results

Ciliary resorption is impaired in an *fls2* mutant that was defective in a gene encoding a CDK-like kinase

Addition of sodium pyrophosphate (NaPPi) to the *Chlamydomonas* cell cultures induces gradual cilia shortening or cilia resorption but not deciliation [23, 34], which provides an excellent system to screen for mutants defective in cilia resorption. In this study, we generated an *AphVIII* DNA insertional mutant, termed flagellar shortening 2 (*fls2)*, which underwent a slow kinetics of ciliary shortening in contrast to wild type cells (Fig. 1A and B). The steady state ciliary length in the mutant and wild type cells was similar (Fig. 1A), indicating that the mutant is only defective in ciliary disassembly but not assembly or ciliary length control. The foreign DNA insert was localized in the last exon of an unknown gene (Cre03.g169500), which encodes a protein kinase of 1106 aa (Fig. 1C). FLS2 is similar to CDK-like protein kinases with a putative cyclin binding domain and a T/S-X-Y motif at the kinase activation loop [35, 36] (Fig. 1D). As expected, phylogenetic analysis has placed FLS2 into the group of CDK-like kinases (Fig. 1E).

To determine whether *FLS2* expression was disrupted in the mutant, we attempted to make antibodies but it was unsuccessful. However, RT-PCR showed that *FLS2* transcript was not detected (Fig. 1F), indicating that foreign DNA insertion likely causes decay of *FLS2* mRNAs. To confirm that disruption of *FLS2* is indeed responsible for the observed ciliary phenotype, HA-tagged *FLS2* was expressed in *fls2* (Fig. 1G). As expected, ciliary shortening defect of *fls2* was rescued (Fig. 1B). Thus, we have identified a CDK-like kinase, FLS2, which functions in ciliary disassembly.

FLS2 regulates ciliary disassembly under physiological conditions and cell cycle progression

To examine whether *fls2* mutation also affects ciliary disassembly under physiological conditions, we first analyzed ciliary shortening during zygotic development [14, 32].

To generate zygotes in *fls2* background, we isolated an mt- strain of *fls2* by crossing the original mt+ *fls2* strain with a wild type mt- strain. As shown in Fig. 2A, ciliary disassembly in *fls2* zygotes was retarded as compared to the wild type control. *Chlamydomonas* cells also disassemble their cilia via gradual ciliary shortening during cell cycle progression [13, 14]. To examine ciliary disassembly in *fls2* during cell cycle progression, cells were synchronized by a light:dark (14h:10h) cycle. Ciliary length was measured during cell cycle progression. As shown in Fig. 2B, ciliary disassembly in *fls2* was retarded as compared to the control. Defects in ciliary disassembly during G1 to S transition has been shown to delay cell cycle progression in mammalian cells as well as in *Chlamydomonas* [13, 16-18]. As expected, *fls2* mutant showed a delay of cell cycle progression (Fig. 2C). Thus, FLS2 is involved in ciliary disassembly under physiological and non-physiological conditions and defects in *FLS2* has physiological consequences.

The kinase activity of FLS2 is required for proper ciliary disassembly and gradually down-regulated by dephosphorylation

Proteins often exhibit gel mobility shift in SDS-PAGE due to changes in the state of protein phosphorylation. To detect possible changes in FLS2 phosphorylation, we analyzed rescued cells expressing FLS2-HA during ciliary shortening induced by NaPPi by immunoblotting. FLS2-HA did not show gel motility shift during the entire course of ciliary disassembly (Fig. 3A). The cell lysates were then analyzed in Phos-tag SDS-PAGE followed by immunoblotting, which has a better separation of phosphoproteins [37, 38]. Before NaPPi treatment (time 0), FLS2-HA exhibited apparently two migrating forms (Fig. 3B). The slower migrating form of FLS2-HA gradually disappeared during ciliary disassembly, indicating that FLS2 is a phosphoprotein in steady state cells and gradually dephosphorylated. Phosphatase treatment confirmed the gel mobility shifts of FLS2-HA were indeed caused by phosphorylation (Fig. 3B).

To examine the relationship between FLS2 phosphorylation and its kinase activity,

153 FLS2-HA was immunoprecipitated from control cells and cells that underwent ciliary
154 disassembly for 180 min followed by *in vitro* kinase assay. The kinase activity of
155 FLS2-HA was greatly decreased at 180 min, indicating that the phosphorylation state
156 of FLS2 correlates with its kinase activity (Fig. 3C). To test whether the kinase activity
157 of FLS2 is required for ciliary disassembly, a kinase-dead version of *FLS2* (*K33R*)
158 tagged with HA was expressed in *fls2* cells. *In vitro* kinase assay showed that *K33R*
159 mutant barely had any kinase activity (Fig. 3C). Examination of the ciliary disassembly
160 kinetics of *K33R* mutant showed that ciliary disassembly defect in *fls2* was not
161 rescued (Fig. 3D). Taken together, these data suggest that FLS2 is an active kinase
162 and gradually down-regulated due to dephosphorylation during ciliary disassembly
163 and its kinase activity is required for proper ciliary disassembly.
164
165 **FLS2 functions in suppressing phosphorylation of CrKinesin13 during early**
166 **stages of ciliary resorption**
167 Next, we were interested in understanding the working mechanism of FLS2 during
168 ciliary disassembly. We examined several factors that have previously been
169 implicated in ciliary disassembly. *Chlamydomonas* aurora-like kinase CALK, which is
170 a homologue of aurora-A, is phosphorylated during and required for ciliary
171 disassembly [7, 23, 39]. To examine whether FLS2 regulates CALK phosphorylation,
172 wild type (WT) and *fls2* cells were induced to shorten their cilia by NaPPi treatment
173 followed by immunoblotting. CALK phosphorylation in *fls2* was not affected as
174 compared to the control (Fig. 4A). Increased trafficking of IFT proteins into cilia occurs
175 during ciliary disassembly and the function of which is not clear [13, 32, 40].
176 Representative IFT proteins IFT121 (IFT-A) and IFT46 (IFT-B) were similarly
177 increased in WT and *fls2* cilia isolated from cells undergoing ciliary disassembly (Fig.
178 4B). Thus, FLS2 is not involved in CALK phosphorylation and increased ciliary
179 trafficking of IFT proteins.
180
181 A single kinesin13 is present in *Chlamdyomonas* and has been shown to be required
182 for ciliary resorption [25]. It is transported from the cell body to cilia upon stimulation

for ciliary disassembly and becomes partially phosphorylated at 60 min after NaPPi treatment [13, 25] (Fig. 4C). We therefore examined whether FLS2 affects the behaviors of CrKinesin13. Immunoblot analysis showed that loss of FLS2 did not affect ciliary transport of CrKinesin13 but lead to early onset of CrKinesin13 phosphorylation already 10 min after adding NaPPi (Fig. 4C). The kinase activity of FLS2 was required for this inhibition as demonstrated by using a kinase-dead mutant *K33R* (Fig. 4D). These data suggest that at least one of the mechanisms of FLS2 in regulation of ciliary disassembly is to suppress CrKinesin13 phosphorylation during the early stage of ciliary resorption.

Previously, we have shown that loss of FLS1 also induces earlier onset of CrKinesin13 phosphorylation and slows ciliary disassembly [13]. Thus, it raises a question whether FLS1 and FLS2 affect each other. FLS1 is phosphorylated upon induction of ciliary disassembly. Immunoblot analysis showed that FLS1 phosphorylation in *fls2* or *K33R* was not altered upon induction of ciliary disassembly (Fig. 4E), indicating that FLS2 does not regulate FLS1 phosphorylation. As shown above in Fig. 3B, FLS2 undergoes dephosphorylation during ciliary disassembly. We examined whether FLS1 affects FLS2 dephosphorylation. To do this, *fls1* cells expressing FLS2-HA were induced for ciliary disassembly followed by Phos-tag immunoblotting. FLS2-HA in *fls1* cells showed similar dephosphorylation relative to the control (Fig. 4F), indicating that FLS1 is not involved in FLS2 dephosphorylation. Thus, the above data suggest that FLS1 and FLS2 do not affect protein phosphorylation of each other.

It was intriguing to learn the ciliary shortening phenotype of an *fls1/fls2* double mutant. However, it was unsuccessful to obtain such a mutant by crossing *fls1* and *fls2*. We decided to deplete FLS1 in *fls2* cells by RNAi as our attempt to knock out *FLS1* by CRISPER/Cas9 failed. RNAi resulted in approximately 80% deletion of FLS1 expression in *fls1-kd/fls2* cells (Fig. 4G). CrKinesin13 was phosphorylated in disassembling cilia of *fls1-kd/fls2* but the degree of its phosphorylation was similar to

213 that in *fls1* or *fls2* single mutant (Fig. 4H)，indicating that FLS1 and FLS2 act in the
214 same pathway to regulate phosphorylation of CrKinesin13. Examination of ciliary
215 disassembly found that *fls1-kd/fls2* cells showed more severe defect in ciliary
216 disassembly than *fls1* or *fls2* alone (Fig. 4I), suggesting critical roles of FLS1 and
217 FLS2 in ciliary disassembly.
218
219 **FLS2 is localized in the cell body and undergoes increased ciliary trafficking**
220 **during ciliary disassembly**
221 To learn more about how FLS2 functions in ciliary disassembly, we determined the
222 cellular distributions of FLS2-HA. Immunostaining showed that FLS2-HA
223 predominantly localized in the cell body (Fig. 5A), which was confirmed by
224 immunoblotting of isolated cell bodies and cilia (Fig. 5B). Interestingly, upon induction
225 of ciliary disassembly, FLS2-HA was transported to cilia (Fig. 5A and B). FLS2-HA in
226 cilia was associated with the axoneme (Fig. 5C). To determine whether transport of
227 FLS2 into cilia upon induction of ciliary disassembly also occurs under physiological
228 conditions, we examined ciliary disassembly during zygotic development.
229 Immunostaining analysis showed that FLS2-HA also increased in cilia of zygotes that
230 underwent ciliary disassembly (Fig. 5D).
231
232 The increase of FLS2 in cilia was rapid. As early as 10 min after induction of ciliary
233 disassembly, the increase of FLS2-HA was detected (Fig. 5C and E). The increased
234 amounts of FLS2-HA in cilia between 10 and 120 min after induction of ciliary
235 disassembly was similar, which is indicative of increased ciliary trafficking of FLS2
236 rather than ciliary accumulation of FLS2 (Fig. 5E). The continuous ciliary trafficking of
237 FLS2 during ciliary disassembly is also supported by the data that the ciliary form of
238 FLS2-HA showed different phosphorylation states during ciliary disassembly, which is
239 similar to the whole cell form of FLS2-HA (Fig. 5E and Fig. 3B). This data also
240 suggests that the phosphorylation state of FLS2 is not involved in ciliary trafficking of
241 FLS2. We further showed that K33R mutant of FLS2 was able to be transported to
242 cilia (Fig. 5F). Thus, FLS2 undergoes increased ciliary trafficking upon induction of

ciliary disassembly and its phosphorylation state and kinase activity are not required for this process. We further showed that ciliary trafficking of FLS2-HA in *fls1* was not affected (Fig. 5G), indicating that FLS1 does not regulate ciliary trafficking of FLS2.

FLS2 is a cargo of IFT70

Though ciliary proteins may diffuse to cilia, IFT appears to be the major mechanism for transporting ciliary proteins into cilia [41-43]. To determine whether IFT was required for FLS2 transport, we took advantage of the temperature conditional kinesin-2 mutant *fla10-1*, in which IFT gradually diminishes at the non-permissive temperature [44, 45]. *fla10-1* cells expressing FLS2-HA were incubated at 22 or 32 ^{o}C for 1 hour followed by addition of NaPPi for 10 min to stimulate ciliary disassembly. The cilia were then isolated for immunoblot analysis. As shown in Fig. 6A, IFT139, FLS2-HA as well as CrKinesin13 were increased in cilia at 22 ^{o}C after stimulation by NaPPi. At 32 ^{o}C， however, IFT protein IFT139 was depleted, and FLS2-HA and CrKinesin13 failed to increase in cilia after NaPPi stimulation. Thus, these results indicate that the transport of FLS2 into cilia depends on IFT.

To identify which IFT proteins may act as cargo adaptors for transport of FLS2, we performed yeast two-hybrid screening by using FLS2 as a bait and each subunit of the IFT complex (IFT-B and IFT-A) as a prey. FLS2 interacted only with IFT70 (Fig. 6B). To determine the minimal segment of FLS2 required for this interaction, a series of deletion mutants were probed for interaction with IFT70 by yeast two-hybrid assay (Fig. 6C). The C-terminal region apart from the kinase domain interacted with IFT70 while the N-terminal region containing the kinase domain did not. Interestingly, various C-terminal segments all showed interaction with IFT70 but with reduced capacity. This data may suggest that the C-terminal non-kinase region as a whole is required for tight interaction with IFT70. To further verify this interaction, a GST pull-down assay was performed. IFT70 was pulled down by the C-terminus of FLS2 (FLS2-CT) tagged with GST (Fig. 6D). Finally, we showed that FLS2 interacts with IFT70 *in vivo* by immunoprecipitation (Fig. 6E).

IFT70 is a protein with 15 tetratricopeptide repeats (TPRs) [46]. To determine the regions of IFT70 that interact with FLS2, various deletion mutants of IFT70 as indicated were tested for interaction with FLS2 by yeast two-hybrid assay (Fig. 6F). It was found that the N-terminal 290 aa region of IFT70 interacted with FLS2. This region has 6 canonical TPRs (no.1-3, 5-6) and two non-canonical TPRs (no.4 and 7) [46]. Deletion of either TPR1, TPR2 or TPR3 abolished the interaction of IFT70 with FLS2 (Fig. 6G), indicating that TPR1-3 form a structural module to mediate this interaction.

Loss of ciliary transport of FLS2 impairs CrKinesin13 phosphorylation and ciliary disassembly

To test whether ciliary transport of FLS2 is required for its function in ciliary disassembly, one strategy would be blocking FLS2 transport by making a mutant of *IFT70* with deletions of TPR1-3. Knockout of *IFT70* in mammalian cells abolishes ciliogenesis, indicating that IFT70 is essential for ciliary assembly [47]. IFT70 tightly interacts with IFT52-IFT88 dimer, which is essential for ciliogenesis [46, 47]. Deletion of TPR1 or TPR1-2 of IFT70 abrogates their interactions with the dimer and could not rescue ciliogenesis in *IFT70* knockout cells [47]. To determine whether TPR1, TPR2 or TPR3 of IFT70 in *Chlamydomonas* functions in interaction with the IFT52-IFT88 dimer, a pulldown assay was performed (Fig. 7A). Full-length of IFT70 and TPR4 deletion mutant could interact with the dimer. However, deletion of either TPR1, TPR2 or TPR3 abolished this interaction. As discussed above, we figured that deletion of these TPRs would block ciliary assembly in live cells and it was not feasible to test ciliary transport of FLS2 by using IFT70 deletion mutants.

Because the C-terminal non-kinase domain of FLS2 was required for its interaction with IFT70 (Fig. 6C), we decided to delete the C-terminus of FLS2 to see whether it affects ciliary transport of FLS2 and ciliary disassembly. HA-tagged C-terminal truncated mutant (Δ CT) of FLS2 was expressed in *fls2* cells (Fig. 7B). Upon induction

303 of ciliary disassembly, the truncated mutant failed to be transported to cilia in contrast
304 to full-length FLS2 (Fig. 7C). *In vitro* kinase assay showed that the △CT mutant did
305 not affect the kinase activity of FLS2 (Fig. 7D), indicating that the C-terminus only
306 functions in ciliary transport. Next, we examined the impact of the C-terminus of FLS2
307 on CrKinesin13 phosphorylation and ciliary disassembly. Similar to *fls2*, loss of
308 C-terminus of FLS2 failed to suppress CrKinesin13 phosphorylation (Fig. 7E) and
309 could not rescue the ciliary disassembly defect of *fls2* (Fig. 7F). These data suggest
310 that transport of FLS2 to cilia regulates CrKinesin13 phosphorylation and ciliary
311 disassembly.
312

Discussion

In this report, we have identified a CDK-like kinase, namely FLS2 that is involved in cilia resorption by a mechanism in which IFT transports FLS2 between the cell body and cilia to control proper phosphorylation of CrKinesin13 in cilia. This study reveals an active role of IFT in regulating ciliary disassembly (resorption) trigged by internal and external cues.

IFT is well established for its function in ciliary assembly and maintenance [27, 28, 48]. However, whether IFT actively functions in ciliary disassembly is not clear. Inactivation of IFT motor kinesin-2 in temperature sensitive mutants of *Chlamydomonas* induces deciliation as well as ciliary shortening [23, 29, 31]. Interestingly, acute ablation of kinesin-2 in mammalian induces ciliary disassembly mainly via deciliation [30]. It is not clear how inactivation of kinesin-2 triggers distinct modes of ciliary disassembly. Nevertheless, these results suggest that down-regulation of IFT may be one of the mechanisms for ciliary disassembly. However, during ciliary resorption triggered by extracellular stimuli or under physiological conditions in *Chlamydomonas*, increased ciliary transport of IFT proteins was observed [25, 32, 33], demonstrating that up-regulation instead of down-regulation of IFT is related to ciliary disassembly. Previously, it has been shown that CrKinesin13 is transported to cilia via IFT during ciliary disassembly [25]. However, it fails to show whether disruption of this transport would impair ciliary disassembly. Our finding that FLS2 is transported by IFT70 to cilia and interruption of this transport impairs ciliary disassembly provides direct evidence for an active role of IFT in ciliary disassembly.

Ciliary resorption entails depolymerization of the axonemal microtubules, which are the backbones of cilia. CrKinesin13 is timely transported to cilia to mediate depolymerization of axonemal microtubules upon induction of cilia resorption [13, 25]. Kinesin13 members KIF2A and KIF24 in mammalian cells are also implicated in cilia resorption [20, 24, 26]. However, they were shown to be localized in the basal body

region, raising the question of how they mediate ciliary disassembly that occurs at the ciliary tip [49]. One may speculate that mammalian kinesin13s may also be transported to cilia during ciliary resorption.

In *Chlamydomonas*, kinesin13 in the cilium becomes partially phosphorylated during later stages of ciliary disassembly [13]. As phosphorylation of CrKinesin13 down-regulates its activity [50], it is proposed that later onset of CrKinesin13 phosphorylation is to ensure constant rate of disassembly because of the polarized nature of the cilium (see discussion in [13]). The regulation of CrKinesin13 phosphorylation is not clear. We have shown here that FLS2, a CDK-like kinase, is timely transported to cilia in a similar manner to CrKinesin13 upon induction of ciliary disassembly. Loss of FLS2 or abrogation of its ciliary transport induces early onset of CrKinesin13 phosphorylation in cilia, suggesting that FLS2 functions in suppressing CrKinesin13 phosphorylation. The later onset of CrKinesin13 phosphorylation in wild type cells can be explained by gradual dephosphorylation and inactivation of FLS2 during ciliary disassembly.

Previously, we have shown that FLS1, another CDK-like kinase, is involved in ciliary disassembly [13]. However, these two kinases exhibit distinct modes of regulation during ciliary disassembly. FLS1 is present both in the cell body and cilia. The cell body form of FLS1 is phosphorylated and activated upon induction of ciliary disassembly to regulate CALK phosphorylation while the cilia form is constitutively phosphorylated. In contrast, FLS2 is a cell body protein. It is gradually inactivated and transported to cilia during cilia resorption. Loss of either FLS1 or FLS2 misregulates CrKinesin13 phosphorylation, suggesting that FLS1 and FLS2 act non-redundantly but collaboratively suppress CrKinesin13 phosphorylation. As FLS1 and FLS2 do not affect each other, they are not in a linear signaling cascade to regulate kinesin13 phosphorylation. The direct targets of FLS1 and FLS2 remain to be identified.

Our finding that FLS2 is involved in ciliary disassembly and cell cycle progression may

374 have implications for functions of human CDKLs in brain development and etiology of
375 related diseases. Patients with mutations in *CDKL2, CDKL3* or *CDKL5* exhibit
376 symptoms in intellectual and developmental disabilities [51, 52]. How defects in ciliary
377 disassembly can cause neuronal developmental disorders? Ciliary disassembly is
378 linked with G1-S transition [17, 18]. Mutated centrosomal-P4.1-associated protein
379 (CPAP) or disruption of WDR62-CEP170-KIF2A pathway causes long cilia, retarded
380 ciliary disassembly, and delayed cell cycle re-entry, leading to premature
381 differentiation of neural progenitors [20, 21]}. Similarly, Tctex-1 also functions in ciliary
382 disassembly and fate determination of neural progenitors [18]. Thus, it is likely that
383 mutations in CDKLs result in defects in ciliary disassembly and cell cycle progression
384 in the brain, leading to mal-differentiation of neural cells.

Materials and Methods

Strains and culture conditions

Chlamydomonas reinhardtii strains *21gr* (mt+; CC-1690) and *6145c* (mt−; CC-1691), available from the *Chlamydomonas* Genetic Center (University of Minnesota). *fls1* and *fls2* mutants (both in *21gr* background) were generated in previous and current studies [13], respectively. Cells were cultured in liquid R medium followed by growth in liquid M medium for 2 - 3 days at 23˚C with aeration under a light/dark (14/10 h) cycle, as reported previously [53]. To induce gamete differentiation, cells were incubated in nitrogen free M medium for 20 hrs under continuous light. Equal number of gametes of opposite mating types were mixed to allow zygote formation.

Cell cycle analysis

Cells were synchronized by growth in M medium in light/dark (14/10 h) cycle with aeration of 5% CO2 in a Light Incubator (Percival AL-36, USA). Cell density was maintained between 10^5 cells/ml and 10^6 cells/ml by dilution into fresh M media at the beginning of each light phase [54]. Cells at the indicated times were fixed with 1% glutaraldehyde followed by scoring cell division microscopically.

Cilia isolation, fractionation and ciliary disassembly

Cilia were isolated after deflagellation by pH shock followed by sucrose gradient purification and fractionated into membrane matrix and axonemal fractions by using 1% NP40 [55]. To induce ciliary disassembly *in vitro*, cell cultures were treated with 20 mM of sodium pyrophosphate (final concentration) for 10 min or indicated time [23, 34]. To examine ciliary disassembly during zygotic development, cells of opposite mating types were induced to undergo gametogenesis in M medium without nitrogen for 20 hrs under continuous light, respectively, followed by mixing to allow mating, zygote formation and development [32]. For zygote formation of cells in *fls2* background, *fls2* (mt+) was crossed with *6145C* (mt-) to generate an mt- *fls2* progeny. Cells were fixed with 1% glutaraldehyde at the indicated times followed by bright field imaging via an inverted Zeiss microscope (Axio Observer Z1, Zeiss) equipped with a

416 charge-coupled device (CCD) camera using a 40 x objective and processed in
417 ImageJ (NIH) and GraphPad Prism (GraphPad, USA). Ciliary length was measured
418 from at least 50 cells. The results are represented as mean ± s.d. For statistical
419 analysis, unpaired two-tailed *t* test was used.
420
421 **Insertional mutagenesis and transgenic strain generation**
422 *fls2* was generated by transformation of *21gr* with a 2.1 kb DNA fragment containing
423 the paromomycin resistance gene *AphVIII* [56]. The disrupted gene was identified by
424 cloning the flanking genomic sequences using RESDA PCR followed by DNA
425 sequencing [56]. To make a construct for expressing *FLS2-HA* in *fls*2 mutant, a full
426 length genomic clone of *FLS2* with endogenous promoter was obtained by PCR from
427 a bacterial artificial chromosome (BAC) containing the *FLS2* gene (BAC 34I11,
428 Clemson University Genomics Institute). A 3xHA tag sequence followed by a Rubisco
429 terminator was cloned from plasmid pKL-3xHA (kindly provided by Karl F. Lechtreck,
430 University of Georgia). The resulting construct was cloned into a modified vector
431 pHyg3 that harbors a hygromycin B resistance gene [57]. *FLS2* deletion and *K33R*
432 mutants were constructed based on the wild type *FLS2* gene construct. The final
433 constructs were linearized with XbaI and transformed into the *fls2* mutant using
434 electroporation.
435
436 **RT-PCR**
437 Total RNA was isolated (HiPure Plant RNA MIni Kit, Magen) and reverse transcribed
438 (The PrimeScript® RT reagent Kit, Takara). Two pairs of primers
439 (5′-GGCAAGAATCATCACGACCAG-3′ and 5′-GTATGCCATGAGGTCGTCCAC-3′)
440 for *FLS2*, and (5′-ATGTGCTGTCCGTGGCTTTC-3′ and
441 5′-GCCCACCAGGTTGTTCTTCA-3′) for *CBLP*, were used for PCR. The amplified
442 fragments were subjected to 1.5% agarose gel electrophoresis.
443
444 **Gene silencing by RNAi**
445 Knockdown of *FLS1* expression in *fls2* mutant was performed by using artificial

446 microRNA (amiRNA) essentially as previously described [58]. The targeted DNA
447 sequence was selected following the instruction in http://wmd3.weigelworld.org.
448 Synthesized oligonucleotides for amiRNA after annealing were cloned into the
449 p3int-RNAi vector at the SpeI/NheI restriction sites [59]. The final construct was
450 linearized with ScaI and transformed by electroporation into *Chlamydomonas*. The
451 targeted sequence: TGCAGGAGCTTAATGTCGCGC. The oligonucleotides: FLS1-F1,
452 CTAGTGCGCGACATTAAGCTTTTGCATCTCGCTGATCGGCACCATGGGGGTGG
453 TGGTGATCAGCGCTATGCAGGAGCTTAATGTCGCGCG; FLS1-R1,
454 CTAGCGCGCGACATTAAGCTCCTGCATAGCGCTGATCACCACCACCCCCATGG
455 TGCCGATCAGCGAGATGCAAAAGCTTAATGTCGCGCA.
456
457 **Primary antibodies**
458 The following antibodies were used for immunoblotting (IB) or immunofluorescence
459 (IF). Rat monoclonal anti-HA (1:50 for IF and 1:1000 for IB; Roche); mouse
460 monoclonal anti-α-tubulin (1:200 for IF and 1:2500 or 1:10,000 for IB; Sigma-Aldrich);
461 rabbit polyclonal anti-CALK (1:10000, IB) (pan 2004); rabbit polyclonal
462 anti-CrKinesin13 (1:3000, IB) [25]; rabbit polyclonal anti-IFT46 (1:2000, IB) [60]; rabbit
463 polyclonal anti-IFT121 (1:2000, IB) [53]; mouse anti-FMG1 (1:5,000 IB) [61]; mouse
464 polyclonal anti-FLS1 (1:1500, IB) [13] and anti-Thiophosphate (1:5000, IB, Abcam).
465 We attempted to make anti-FLS2 antibody in rabbits and mouse by using 641-841 aa
466 and 756-1106 aa as antigens, respectively, but none were successful.
467
468 **Immunoblotting and immunofluorescence**
469 IB and IF experiments were performed as described previously [55]. The secondary
470 antibodies used for IF are the following: Goat anti-Rat IgG Alexa Fluor 488, Goat
471 anti-Mouse IgG Alexa Fluor 594. Cells were analyzed under a Zeiss LSM780 META
472 Observer Z1 Confocal Laser Microscope and the images were acquired and
473 processed by ZEN 2012 Light Edition (Zeiss). The images were processed in Adobe
474 Photoshop and assembled in Adobe Illustrator (Adobe).
475

476 **Phosphatase treatment and Phos-tag SDS-PAGE**

477 Cell samples (5x10^6 cells) were lysed in 40 μl Buffer (50 mM Tris pH 7.5, 10 mM
478 $MgCl_2$) containing protease inhibitor cocktail and 25 μg/ml ALLN. For phosphatase
479 treatment, the final 50 μl reaction buffer contained 38 μl of cell lysate, 2 μl lambda
480 protein phosphatase (800 U) and buffer components as instructed (Sigma) and the
481 reaction was terminated after 30 min at 30 °C. To visualize protein phosphorylation by
482 gel mobility shift, proteins were separated in phos-tag gel system [38]. A 6%
483 SDS-PAGE with 20 mM Phos-tag acrylamide (Wako) was used. After electrophoresis,
484 the divalent cations were removed from the Phos-tag gels by incubating them with
485 transfer buffer containing 2 mM EDTA for 20 min before membrane transferring.

486

487 **Immunoprecipitation (IP) and *in vitro* protein kinase assay**

488 1×10^9 cells were lysed in IP buffer (20 mM Hepes, pH 7.2, 5 mM $MgCl_2$, 1 mM DTT, 1
489 mM EDTA, 150 mM NaCl, EDTA-free protease inhibitor cocktail, 25 μg/ml ALLN). For
490 IP with isolated cilia, 1 mg cilia were lysed in IP buffer supplemented with 0.6 M KCl
491 and 0.05 M CaCl2. The lysates were incubated with 30 μl pre-washed rat anti-HA
492 Affinity Matrix (Roche) for 3 h at 4˚C, followed by washing three times with IP buffer
493 containing 0.1% NP40 and 0.1% Triton X-100 and centrifugation. For *in vitro* protein
494 kinase assay, it was performed with ATPγS as a phosphodonor and
495 anti-thiophosphate ester antibody to detect substrate phosphorylation [62]. The
496 immunoprecipitates of FLS2-HA were incubated at room temperature for 30 min in 30
497 μl reaction buffer (10 mM HEPES pH 7.2, 150 mM NaCl, 10 mM $MgCl_2$, 5 mM DTT, 2
498 μg MBP and 1 mM ATPγS (Abcam)), followed by addition of 1.5 μl of 50 mM
499 p-nitrobenzylmesylate (Abcam) for 2 h. Protein phosphorylation was detected by
500 immunoblotting with anti-thiophosphate ester antibody.

501

502 **Yeast-based two-hybrid analysis**

503 cDNAs of *FLS2* and IFT genes cloned by PCR from a *Chlamydomonas* cDNA library
504 were cloned into yeast expression vectors pGBKT7 and pGADT7, respectively. The
505 resulting constructs were co-transformed into AH109 yeast cells with different

506 combinations. The transformants were grown at 30 °C for 2 - 3 days on selection
507 medium SD lacking leucine, tryptophan, histidine, and adenine (SD, -Leu, -Trp, -His,
508 -Ade) or lacking leucine and tryptophan (SD, -Leu, -Trp).
509
510 **Pull-down assays**
511 *GST-FLS2-CT*$_{290-1106}$ and *GST-IFT52* were cloned into bacterial expression vector
512 pGEX-6P-1, respectively. IFT88-His, IFT70-His and various His-tagged IFT70
513 deletion mutants were cloned into bacterial expression vector pET28a, respectively.
514 The proteins were expressed in BL21 cells. For pull-down assay of GST-FLS2-CT
515 and IFT70-His, these two proteins were co-expressed. For pull-down assays of IFT70
516 or its variants with IFT88-His and GST-IFT52, IFT70 and its variants were separately
517 expressed while IFT88-His and GST-IFT52 were co-expressed. The cell lysates were
518 mixed as indicated followed by pull-down and immunoblotting.
519

ACKNOWLEDGMENTS

We are grateful to Drs. Robert Bloodgood, Kaiyao Huang and Karl Lechtreck for providing antibodies and/or plasmids. We thank previous laboratory members for preliminary data. We also thank the Core Facility of the Center for Biomedical Analysis (Tsinghua University) for assistance on cell imaging analysis. This work was supported by the National Key R&D Program of China (2018YFA0902500, 2017YFA0503500) and the National Natural Science Foundation of China (31671387 and 31972888) (to J.P.).

Contributions

Q.Z. S.L. S.S. Z.W. and J.P. designed the experiments and analyzed the data; Q.Z. S.L. S.S. and Z.W. performed research; J.P. contributed reagents and analytic tools; J.P. and Q.Z. wrote the paper.

Competing financial interests

The authors declare no conflict of interest.

References

1. Anvarian Z, Mykytyn K, Mukhopadhyay S, Pedersen LB, Christensen ST. Cellular signalling by primary cilia in development, organ function and disease. Nat Rev Nephrol. 2019;15:199-219.
2. Spassky N, Meunier A. The development and functions of multiciliated epithelia. Nat Rev Mol Cell Biol. 2017;18:423-436.
3. Reiter JF, Leroux MR. Genes and molecular pathways underpinning ciliopathies. Nat Rev Mol Cell Biol. 2017;18:533-547.
4. Phua SC, Chiba S, Suzuki M, Su E, Roberson EC, Pusapati GV, et al. Dynamic Remodeling of Membrane Composition Drives Cell Cycle through Primary Cilia Excision. Cell. 2017;168:264-279 e215.
5. Rieder CL, Jensen CG, Jensen LC. The resorption of primary cilia during mitosis in a vertebrate (PtK1) cell line. J Ultrastruct Res. 1979;68:173-185.
6. Tucker RW, Scher CD, Stiles CD. Centriole deciliation associated with the early response of 3T3 cells to growth factors but not to SV40. Cell. 1979;18:1065-1072.
7. Pugacheva EN, Jablonski SA, Hartman TR, Henske EP, Golemis EA. HEF1-dependent Aurora A activation induces disassembly of the primary cilium. Cell. 2007;129:1351-1363.
8. Liang Y, Meng D, Zhu B, Pan J. Mechanism of ciliary disassembly. Cell Mol Life Sci. 2016;73:1787-1802.
9. Hsu KS, Chuang JZ, Sung CH. The Biology of Ciliary Dynamics. Cold Spring Harb Perspect Biol. 2017;9.
10. Korobeynikov V, Deneka AY, Golemis EA. Mechanisms for nonmitotic activation of Aurora-A at cilia. Biochem Soc Trans. 2017;45:37-49.
11. Quarmby LM. Cellular deflagellation. Int Rev Cytol. 2004;233:47-91.
12. Bloodgood RA. Resorption of organelles containing microtubules. Cytobios. 1974;9:142-161.
13. Hu Z, Liang Y, He W, Pan J. Cilia disassembly with two distinct phases of regulation. Cell Rep. 2015;10:1803-1810.
14. Cavalier-Smith T. Basal body and flagellar development during the vegetative cell cycle and the sexual cycle of Chlamydomonas reinhardii. J Cell Sci. 1974;16:529-556.
15. Mirvis M, Siemers KA, Nelson WJ, Stearns TP. Primary cilium loss in mammalian cells occurs predominantly by whole-cilium shedding. PLoS Biol. 2019;17:e3000381.
16. Izawa I, Goto H, Kasahara K, Inagaki M. Current topics of functional links between primary cilia and cell cycle. Cilia. 2015;4:12.
17. Kim S, Zaghloul NA, Bubenshchikova E, Oh EC, Rankin S, Katsanis N, et al. Nde1-mediated inhibition of ciliogenesis affects cell cycle re-entry. Nat Cell Biol. 2011;13:351-360.
18. Li A, Saito M, Chuang JZ, Tseng YY, Dedesma C, Tomizawa K, et al. Ciliary transition zone activation of phosphorylated Tctex-1 controls ciliary resorption, S-phase entry and fate of neural progenitors. Nat Cell Biol. 2011;13:402-411.
19. Jackson PK. Do cilia put brakes on the cell cycle? Nat Cell Biol. 2011;13:340-342.
20. Zhang W, Yang SL, Yang M, Herrlinger S, Shao Q, Collar JL, et al. Modeling microcephaly with cerebral organoids reveals a WDR62-CEP170-KIF2A pathway promoting cilium disassembly in neural progenitors. Nat Commun. 2019;10:2612.
21. Gabriel E, Wason A, Ramani A, Gooi LM, Keller P, Pozniakovsky A, et al. CPAP promotes timely cilium disassembly to maintain neural progenitor pool. EMBO J. 2016;35:803-819.
22. Eguether T, Hahne M. Mixed signals from the cell's antennae: primary cilia in cancer. EMBO Rep.

583 2018;19.
584 23. Pan J, Wang Q, Snell WJ. An aurora kinase is essential for flagellar disassembly in
585 Chlamydomonas. Dev Cell. 2004;6:445-451.
586 24. Miyamoto T, Hosoba K, Ochiai H, Royba E, Izumi H, Sakuma T, et al. The
587 Microtubule-Depolymerizing Activity of a Mitotic Kinesin Protein KIF2A Drives Primary Cilia
588 Disassembly Coupled with Cell Proliferation. Cell Rep. 2015;10:664-673.
589 25. Piao T, Luo M, Wang L, Guo Y, Li D, Li P, et al. A microtubule depolymerizing kinesin
590 functions during both flagellar disassembly and flagellar assembly in Chlamydomonas. Proc Natl Acad
591 Sci U S A. 2009;106:4713-4718.
592 26. Kim S, Lee K, Choi JH, Ringstad N, Dynlacht BD. Nek2 activation of Kif24 ensures cilium
593 disassembly during the cell cycle. Nat Commun. 2015;6:8087.
594 27. Scholey JM. Intraflagellar transport. Annu Rev Cell Dev Biol. 2003;19:423-443.
595 28. Rosenbaum JL, Witman GB. Intraflagellar transport. Nat Rev Mol Cell Biol. 2002;3:813-825.
596 29. Lux FG, 3rd, Dutcher SK. Genetic interactions at the FLA10 locus: suppressors and synthetic
597 phenotypes that affect the cell cycle and flagellar function in Chlamydomonas reinhardtii. Genetics.
598 1991;128:549-561.
599 30. Engelke MF, Waas B, Kearns SE, Suber A, Boss A, Allen BL, et al. Acute Inhibition of
600 Heterotrimeric Kinesin-2 Function Reveals Mechanisms of Intraflagellar Transport in Mammalian
601 Cilia. Curr Biol. 2019;29:1137-1148 e1134.
602 31. Mueller J, Perrone CA, Bower R, Cole DG, Porter ME. The FLA3 KAP subunit is required for
603 localization of kinesin-2 to the site of flagellar assembly and processive anterograde intraflagellar
604 transport. Mol Biol Cell. 2005;16:1341-1354.
605 32. Pan J, Snell WJ. Chlamydomonas shortens its flagella by activating axonemal disassembly,
606 stimulating IFT particle trafficking, and blocking anterograde cargo loading. Dev Cell.
607 2005;9:431-438.
608 33. Wang L, Gu L, Meng D, Wu Q, Deng H, Pan J. Comparative Proteomics Reveals Timely
609 Transport into Cilia of Regulators or Effectors as a Mechanism Underlying Ciliary Disassembly. J
610 Proteome Res. 2017;16:2410-2418.
611 34. Lefebvre PA, Nordstrom SA, Moulder JE, Rosenbaum JL. Flagellar elongation and shortening in
612 Chlamydomonas. IV. Effects of flagellar detachment, regeneration, and resorption on the induction of
613 flagellar protein synthesis. J Cell Biol. 1978;78:8-27.
614 35. Endicott JA, Noble ME. Structural characterization of the cyclin-dependent protein kinase family.
615 Biochem Soc Trans. 2013;41:1008-1016.
616 36. Yee KW, Moore SJ, Midmer M, Zanke BW, Tong F, Hedley D, et al. NKIAMRE, a novel
617 conserved CDC2-related kinase with features of both mitogen-activated protein kinases and
618 cyclin-dependent kinases. Biochem Biophys Res Commun. 2003;308:784-792.
619 37. Horinouchi T, Terada K, Higashi T, Miwa S. Using Phos-Tag in Western Blotting Analysis to
620 Evaluate Protein Phosphorylation. Methods Mol Biol. 2016;1397:267-277.
621 38. Kinoshita E, Kinoshita-Kikuta E, Takiyama K, Koike T. Phosphate-binding tag, a new tool to
622 visualize phosphorylated proteins. Mol Cell Proteomics. 2006;5:749-757.
623 39. Cao M, Meng D, Wang L, Bei S, Snell WJ, Pan J. Activation loop phosphorylation of a protein
624 kinase is a molecular marker of organelle size that dynamically reports flagellar length. Proc Natl Acad
625 Sci U S A. 2013;110:12337-12342.
626 40. Qin H, Diener DR, Geimer S, Cole DG, Rosenbaum JL. Intraflagellar transport (IFT) cargo: IFT

627 transports flagellar precursors to the tip and turnover products to the cell body. J Cell Biol.
628 2004;164:255-266.
629 41. Wingfield JL, Lechtreck KF, Lorentzen E. Trafficking of ciliary membrane proteins by the
630 intraflagellar transport/BBSome machinery. Essays Biochem. 2018;62:753-763.
631 42. Lechtreck KF. IFT-Cargo Interactions and Protein Transport in Cilia. Trends Biochem Sci.
632 2015;40:765-778.
633 43. Kee HL, Dishinger JF, Blasius TL, Liu CJ, Margolis B, Verhey KJ. A size-exclusion permeability
634 barrier and nucleoporins characterize a ciliary pore complex that regulates transport into cilia. Nat Cell
635 Biol. 2012;14:431-437.
636 44. Walther Z, Vashishtha M, Hall JL. The Chlamydomonas FLA10 gene encodes a novel
637 kinesin-homologous protein. J Cell Biol. 1994;126:175-188.
638 45. Kozminski KG, Beech PL, Rosenbaum JL. The Chlamydomonas kinesin-like protein FLA10 is
639 involved in motility associated with the flagellar membrane. J Cell Biol. 1995;131:1517-1527.
640 46. Taschner M, Kotsis F, Braeuer P, Kuehn EW, Lorentzen E. Crystal structures of IFT70/52 and
641 IFT52/46 provide insight into intraflagellar transport B core complex assembly. J Cell Biol.
642 2014;207:269-282.
643 47. Takei R, Katoh Y, Nakayama K. Robust interaction of IFT70 with IFT52-IFT88 in the IFT-B
644 complex is required for ciliogenesis. Biol Open. 2018;7.
645 48. Taschner M, Lorentzen E. The Intraflagellar Transport Machinery. Cold Spring Harb Perspect
646 Biol. 2016;8.
647 49. Marshall WF, Rosenbaum JL. Intraflagellar transport balances continuous turnover of outer
648 doublet microtubules: implications for flagellar length control. J Cell Biol. 2001;155:405-414.
649 50. Wang L, Piao T, Cao M, Qin T, Huang L, Deng H, et al. Flagellar regeneration requires
650 cytoplasmic microtubule depolymerization and kinesin-13. J Cell Sci. 2013;126:1531-1540.
651 51. Dubos A, Pannetier S, Hanauer A. Inactivation of the CDKL3 gene at 5q31.1 by a balanced t(X;5)
652 translocation associated with nonspecific mild mental retardation. Am J Med Genet A.
653 2008;146A:1267-1279.
654 52. Kilstrup-Nielsen C, Rusconi L, La Montanara P, Ciceri D, Bergo A, Bedogni F, et al. What we
655 know and would like to know about CDKL5 and its involvement in epileptic encephalopathy. Neural
656 Plast. 2012;2012:728267.
657 53. Zhu B, Zhu X, Wang L, Liang Y, Feng Q, Pan J. Functional exploration of the IFT-A complex in
658 intraflagellar transport and ciliogenesis. PLoS Genet. 2017;13:e1006627.
659 54. Bisova K, Krylov DM, Umen JG. Genome-wide annotation and expression profiling of cell cycle
660 regulatory genes in Chlamydomonas reinhardtii. Plant Physiol. 2005;137:475-491.
661 55. Zhu X, Liang Y, Gao F, Pan J. IFT54 regulates IFT20 stability but is not essential for tubulin
662 transport during ciliogenesis. Cell Mol Life Sci. 2017;74:3425-3437.
663 56. Meng D, Cao M, Oda T, Pan J. The conserved ciliary protein Bug22 controls planar beating of
664 Chlamydomonas flagella. J Cell Sci. 2014;127:281-287.
665 57. Berthold P, Schmitt R, Mages W. An engineered Streptomyces hygroscopicus aph 7" gene
666 mediates dominant resistance against hygromycin B in Chlamydomonas reinhardtii. Protist.
667 2002;153:401-412.
668 58. Liang Y, Pan J. Regulation of flagellar biogenesis by a calcium dependent protein kinase in
669 Chlamydomonas reinhardtii. PLoS One. 2013;8:e69902.
670 59. Molnar A, Bassett A, Thuenemann E, Schwach F, Karkare S, Ossowski S, et al. Highly specific

671 gene silencing by artificial microRNAs in the unicellular alga Chlamydomonas reinhardtii. Plant J.
672 2009;58:165-174.
673 60. Lv B, Wan L, Taschner M, Cheng X, Lorentzen E, Huang K. Intraflagellar transport protein
674 IFT52 recruits IFT46 to the basal body and flagella. J Cell Sci. 2017;130:1662-1674.
675 61. Bloodgood RA, Salomonsky NL. The transmembrane signaling pathway involved in directed
676 movements of Chlamydomonas flagellar membrane glycoproteins involves the dephosphorylation of a
677 60-kD phosphoprotein that binds to the major flagellar membrane glycoprotein. J Cell Biol.
678 1994;127:803-811.
679 62. Allen JJ, Li M, Brinkworth CS, Paulson JL, Wang D, Hubner A, et al. A semisynthetic epitope for
680 kinase substrates. Nat Methods. 2007;4:511-516.
681

683 **Figure legends**

684 **Figure 1. Identification of a CDK-like kinase, FLS2 that functions in ciliary**
685 **disassembly.**

686 (A) *fls2* mutant is defective in cilia resorption but not steady state ciliary length. Wild
687 type (WT) or *fls2* cells were treated with or without 20 mM NaPPi for three hours
688 followed by ciliary length measurement. Ciliary length data shown here and below are
689 presented as mean±SD with n = 50 cilia. N.S., not significant (p>0.05).

690 (B) *fls2* mutant exhibits slower kinetics of ciliary disassembly. WT, *fls2* and the
691 rescued cells were induced for ciliary disassembly by addition of 20 mM NaPPi.
692 Ciliary length was measured at the indicated times.

693 (C) Diagrams of the gene structure of *FLS2* with the indicated foreign DNA insertion
694 site and the domain structure of the protein kinase encoded by *FLS2*. The *AphVIII*
695 DNA fragment is inserted in the last exon of *FLS2* between 3353 and 3354 nt and
696 results in deletion of the 3352 nt. The left and right arrows show the positions of the
697 primers used for RT-PCR.

698 (D) Alignment of the protein kinase domain III and VIII of FLS2 with those of human
699 CDK1，CDK-like kinases (CDKLs) and two *Chlamydomonas* CDKLs (LF5 and FLS1)
700 that are implicated in ciliary functions.

701 (E) Phylogenetic analysis places FLS2 in the group of CDKLs. A neighbor-joining
702 phylogenetic tree was constructed by using an algorithm (www.phylogeny.fr) following
703 the instruction. FLS2 was analyzed with the human CDKLs and two
704 *Chlamdydomonas* CDKLs: FLS1 and LF5. The outgroup members include LF2 and
705 LF4, two MAPK-related kinases in *Chlamdyomonas*; CDPK1, a *Chlamydomonas*
706 calcium dependent kinase and HsCDK1, a cyclin-dependent kinase. The numbers
707 above the line indicate the bootstrap values. The sequences of the kinase domains
708 were used for the analysis.

709 (F) *FLS2* is not expressed in *fls2* cells shown by RT-PCR. Gene expression of *CBLP*
710 was used as a control.

711 (G) An immunoblot showing expression of *FLS2-HA* in *fls2* cells. WT and *fls2* cells
712 were used as controls.

Figure 2. *FLS2* regulates ciliary disassembly under physiological conditions and cell cycle progression.

(A) *fls2* is defective in ciliary disassembly during zygote development. Gametes of opposite mating types of *fls2* were mixed to allow mating and zygote development followed by ciliary length measurement. The mating of wild type gametes was used as a control. Error bars indicate SD.

(B) *fls2* is defective in ciliary disassembly during cell cycle progression. WT, *fls2* and rescued cells were synchronized by a light/dark (14h/10h) cycle. Ciliary length was scored beginning in the dark period when cells prepared to enter mitosis.

(C) Cell cycle progression in *fls2* mutant is retarded. Dividing cells were scored microscopically in the dark period of the light/dark cycle. Compared to WT and rescued cells, the peak of cell division in *fls2* mutant was delayed around 3 hrs.

Figure 3. FLS2 kinase activity is required for ciliary disassembly during which it undergoes dephosphorylation and inactivation

(A) *FLS2* expression is not altered during ciliary disassembly. *fls2* rescued cells expressing *FLS2-HA* was induced for ciliary disassembly by addition of NaPPi followed by immunoblotting with the indicated antibodies.

(B) FLS2 undergoes gradual dephosphorylation during ciliary disassembly. A phos-tag immunoblotting was performed using antibodies as indicated. Steady state cells were treated with or without phosphatase (Ptase) to demonstrate that the gel mobility shift was caused by changes in protein phosphorylation.

(C) Dephosphorylation of FLS2 results in loss of its kinase activity. *fls2* cells expressing wild type *FLS2-HA* or kinase dead mutant *K33R-HA* were treated with 20 mM NaPPi for the indicated times. Wild type (WT) cells were used as a negative control. Cell lysates were incubated with anti-HA antibodies for immunoprecipitation followed by *in vitro* kinase assay. ATPγS was used as ATP donor and myelin basic protein as substrate. Anti-thiophosphate ester antibody was used to detect substrate phosphorylation.

743 (D) The kinase activity of FLS2 is required for ciliary disassembly. Cells from WT, *fls2*
744 and kinase-dead mutant *K33R* were induced for ciliary disassembly by NaPPi
745 treatment. Ciliary length was measured at the indicated times. Bars indicate SD.
746
747 **Figure 4. FLS2 does not regulate CALK and IFT but suppresses CrKinesin13**
748 **phosphorylation independently of FLS1.**
749 (A) CALK phosphorylation is not affected in *fls2*. WT and *fls2* cells were treated with
750 NaPPi for ciliary disassembly. Cell lysates at the indicated time were analyzed by
751 immunoblotting with CALK antibody. CALK underwent phosphorylation with slower
752 gel migration, which were not affected in *fls2*.
753 (B) FLS2 does not affect increasing transport of IFT proteins in cilia. WT or *fls2* Cells
754 were treated with or without 20 mM NaPPi for 10 min followed by cilia isolation and
755 immunoblotting. IFT121, a subunit of IFT-A and IFT46, a subunit of IFT-B were
756 analyzed. α-tubulin was used as a loading control.
757 (C) Loss of FLS2 does not affect ciliary transport of CrKinesin13 but induces earlier
758 onset of its phosphorylation. WT or *fls2* cells were treated with NaPPi for the indicated
759 times followed by cilia isolation and immunoblotting. The slower migration form of
760 CrKinesin13 is due to phosphorylation as demonstrated previously.
761 (D) The kinase activity of FLS2 is required for suppression of earlier onset of
762 CrKinesin13 phosphorylation. Isolated cilia from cell samples that were treated with or
763 without NaPPi for 10 min were subjected to immunoblot analysis with the indicated
764 antibodies.
765 (E) FLS1 phosphorylation is not altered in *fls2*. Cell samples as indicated were
766 analyzed by immunoblotting with FLS1 antibody.
767 (F) FLS2 phosphorylation is not altered in *fls1*. *fls1* or *fls2* cells expressing FLS2-HA
768 were treated for the indicated times followed by Phos-tag immunoblotting. FLS2
769 phosphorylation as evidenced by patterns of gel migration was similar between *fls1*
770 and *fls2* cells.
771 (G) Generation of an *fls1-kd/fls2* strain by RNAi depletion of FLS1 in *fls2* cells. Cell
772 samples as indicated were subjected to immunoblotting with anti-FLS1 antibody.

(H) CrKinesin13 phosphorylation in *fls1-kd/fls2* cells. Cilia were isolated from cell samples that were treated with NaPPi for 10 min and were then subjected to immunoblotting.

(I) *fls1-kd/fls2* cells show more severe defect in ciliary disassembly. Cells as indicated were induced for ciliary disassembly followed by ciliary length measurement at the indicated times. Bars indicate SD.

Figure 5. Increased ciliary trafficking of FLS2 upon induction of ciliary disassembly

(A) FLS2 is a cell body protein and transported to cilia during ciliary disassembly as examined by immunostaining. *fls2* cells expressing *FLS2-HA* were treated with or without NaPPi for 10 min followed by immunostaining with HA and α-tubulin antibodies. WT cells were used as control. Bar, 5 μm.

(B) Analysis of ciliary transport of FLS2 by immunoblotting. *fls2* cells expressing *FLS2-HA* were separated into cell bodies (CB) and cilia (C) fractions after treatment with or without NaPPi for 10 min followed by immunoblotting. WC, whole cells.

(C) Ciliary FLS2 is associated with the axonemes. Cilia isolated from cells treated with or without NaPPi for 10 min were fractionated into membrane matrix (M+M) and axonemal fractions followed by immunoblotting with the indicated antibodies. FMG1, a ciliary membrane protein was used as a control for M+M fractions.

(D) FLS2 is transported to cilia during ciliary disassembly in zygote development. Immunostaining analysis of FLS2 in mt+ and mt- gametes (G+ and G-), 0.5 hr (Z0.5h) and 2.5 hr (Z2.5h) zygotes. Bar, 5 μm.

(E) FLS2 in cilia undergoes dephosphorylation during ciliary disassembly but its levels are unchanged. Cilia were isolated from cells treated with NaPPi for 10 or 120 min. The isolated cilia were treated with or without phosphatase (Ptase) followed by phos-tag immunoblotting. Please note that FLS2 in the 10 min sample without phosphatase treatment exhibited slower gel motility shift relative to other samples.

(F) The kinase activity of FLS2 is not required for its ciliary transport. Whole cells (WC) or isolated cilia from kinase-dead *K33R* mutant cells treated with or without NaPPi for

10 min were subjected to immunoblot analysis.

(G) FLS1 does not affect ciliary transport of FLS2. Cilia isolated from *fls1* cells expressing FLS2-HA treated with or without NaPPi were analyzed by phos-tag immunoblotting. *fls2* cells expressing *FLS2-HA* were used as control. Ciliary transport as well as gel mobility of FLS2 expressed in *fls1* were similar to the control.

Figure 6. FLS2 is a cargo of IFT70 for ciliary transport

(A) Ciliary transport of FLS2 depends on IFT. Temperature sensitive mutant *fla10-1* cells expressing FLS2-HA were incubated at the indicated temperatures for 1h followed by treatment with NaPPi or not for 10 min. The cilia were then isolated for immunoblotting with the indicated antibodies.

(B) FLS2 interacts with IFT70 shown in yeast two-hybrid assays. Subunits of IFT-B or IFT-A were transformed respectively into yeast cells with FLS2, followed by growth on selection medium lacking Leu and Trp (-2) or Leu, Trp, His and Ade (-4).

(C-D) The C-terminal non-kinase region of FLS2 is required for its interaction with IFT70. Full-length FLS2 and its deletion variants were assayed for their interaction with IFT70 in yeast two-hybrid assays (C). A GST pull-down assay of bacterial expressed FLS2-CT and IFT70 (D).

(E) FLS2 interacts with IFT70 in vivo shown by immunoprecipitation. Cilia were isolated from control cells (WT) or *fls2* cells expressing FLS2-HA during ciliary disassembly followed by immunoprecipitation with anti-HA antibody and immunoblotting.

(F-G) TPR1-3 of IFT70 is essential for its interaction with FLS2. Full-length of IFT70 and its various segments (E) or various TPR deletion mutants (F) were subjected to yeast two-hybrid assays with FLS2.

Figure 7. The C-terminal non-kinase region of FLS2 is required for its ciliary transport and proper ciliary disassembly.

(A) Deletion of TPR1, TPR2 or TPR3 of IFT70 abrogates its interaction with IFT52-IFT88 dimer. Cell lysates from bacterial cells expressing His-tagged full-length

833 *IFT70* and its various deletion mutants (IFT70*-His) were mixed, respectively, with cell
834 lysates from cells expressing GST-IFT52 and IFT88-His followed by GST pull-down
835 assay. His and GST antibodies were used for immunoblotting.
836 (B) Expression of C-terminal deletion mutant of *FLS2* in *fls2* cells. *fls2* cells
837 expressing HA-tagged full-length (FL) *FLS2* or its C-terminal deletion mutants (Δ CT)
838 (three strains 11, 109, 191) were analyzed by immunoblotting. *fls2* cells were used as
839 a negative control.
840 (C) The C-terminal region of FLS2 is required for its ciliary transport. Cilia were
841 isolated from *fls2* cells expressing full-length *FLS2* or Δ CT mutant that were treated
842 with or without NaPPi for 10 min followed by immunoblot analysis.
843 (D) The C-terminal region of FLS2 does not affect its kinase activity. FLS2 was
844 immunoprecipitated with anti-HA from cell samples as indicated and subjected to
845 immunoblot analysis and in vitro kinase assay. *In vitro* kinase assay was performed
846 as shown in Fig. 3C.
847 (E-F) Failed ciliary transport of FLS2 by C-terminal deletion induces CrKinesin13
848 phosphorylation and impairs ciliary disassembly. Cilia isolated from cell samples as
849 indicated were analyzed by immunoblotting (E). *fls2* cells expressing full-length (FL)
850 *FLS2* or Δ CT mutant were induced for ciliary disassembly by NaPPi treatment
851 followed by ciliary length measurement at the indicated times. *fls2* cells were used as
852 control. Bars indicate SD.

Figure 1 Zhao et al.,

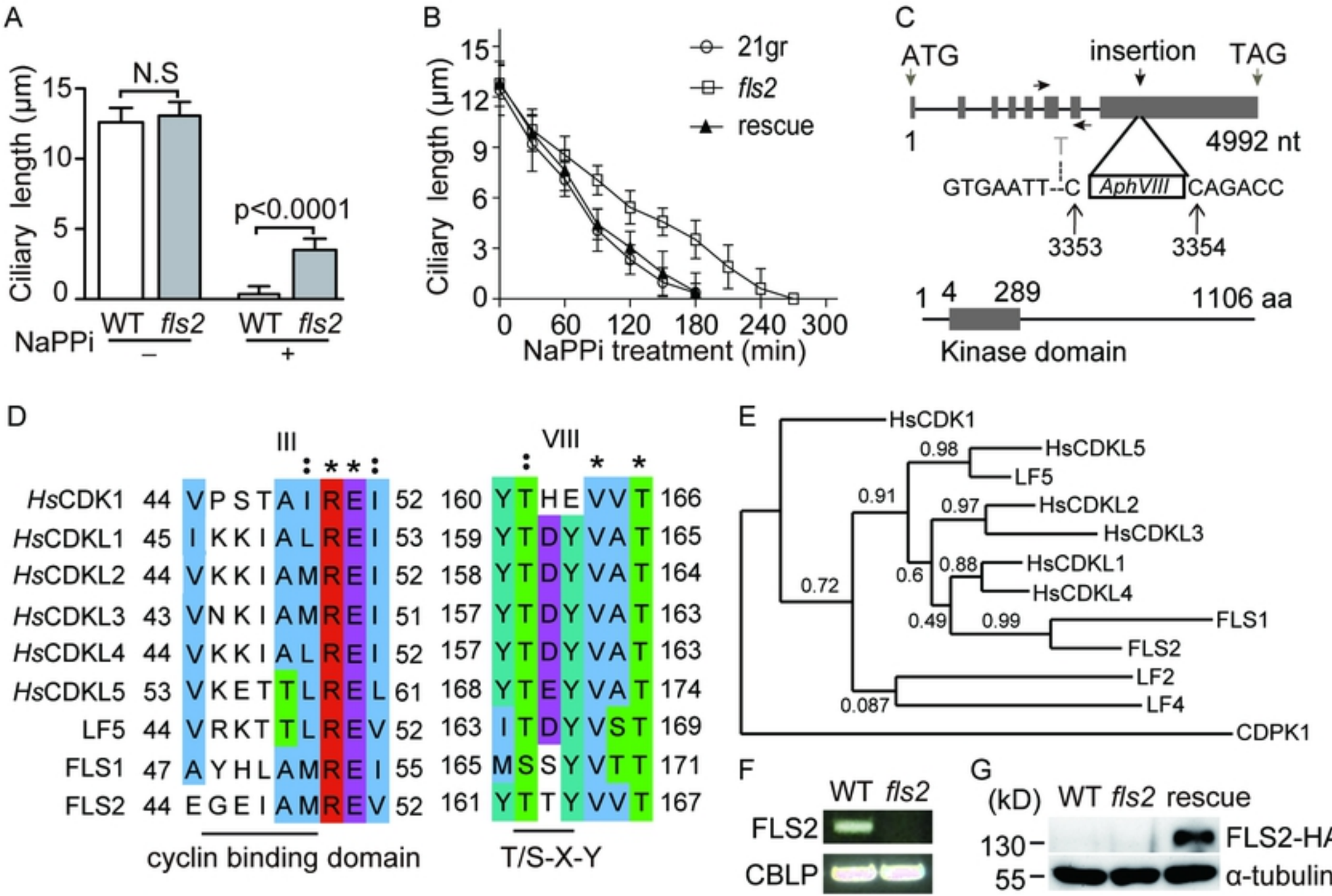

Figure1

Figure 2 Zhao et al.,

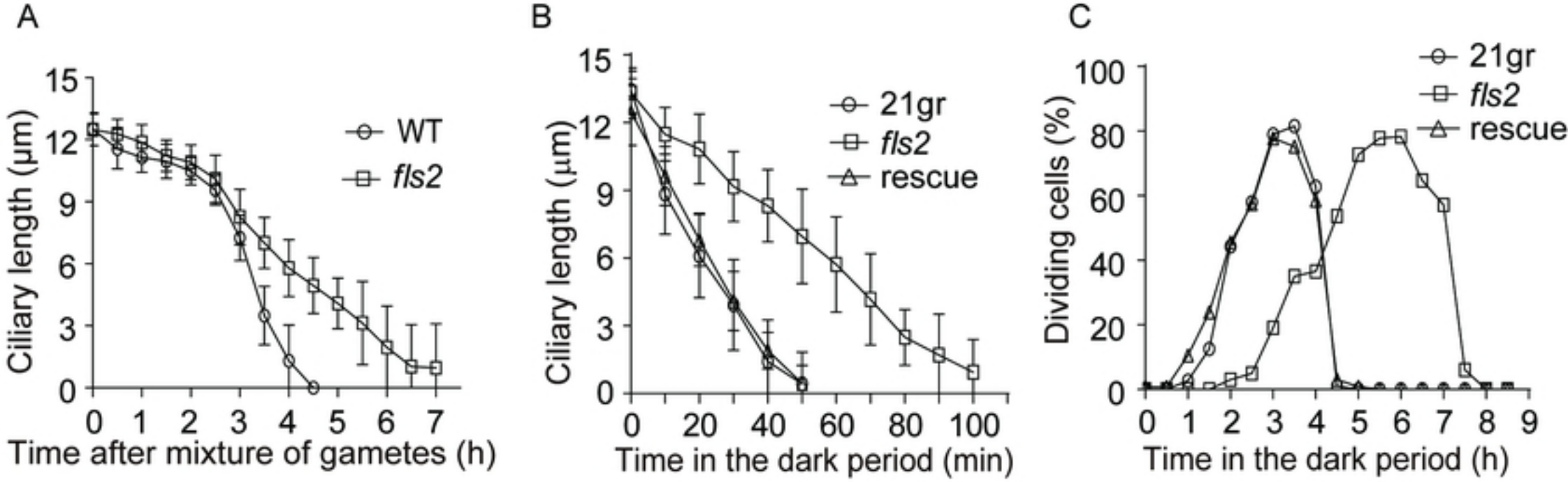

Figure2

Figure 3 Zhao et al.,

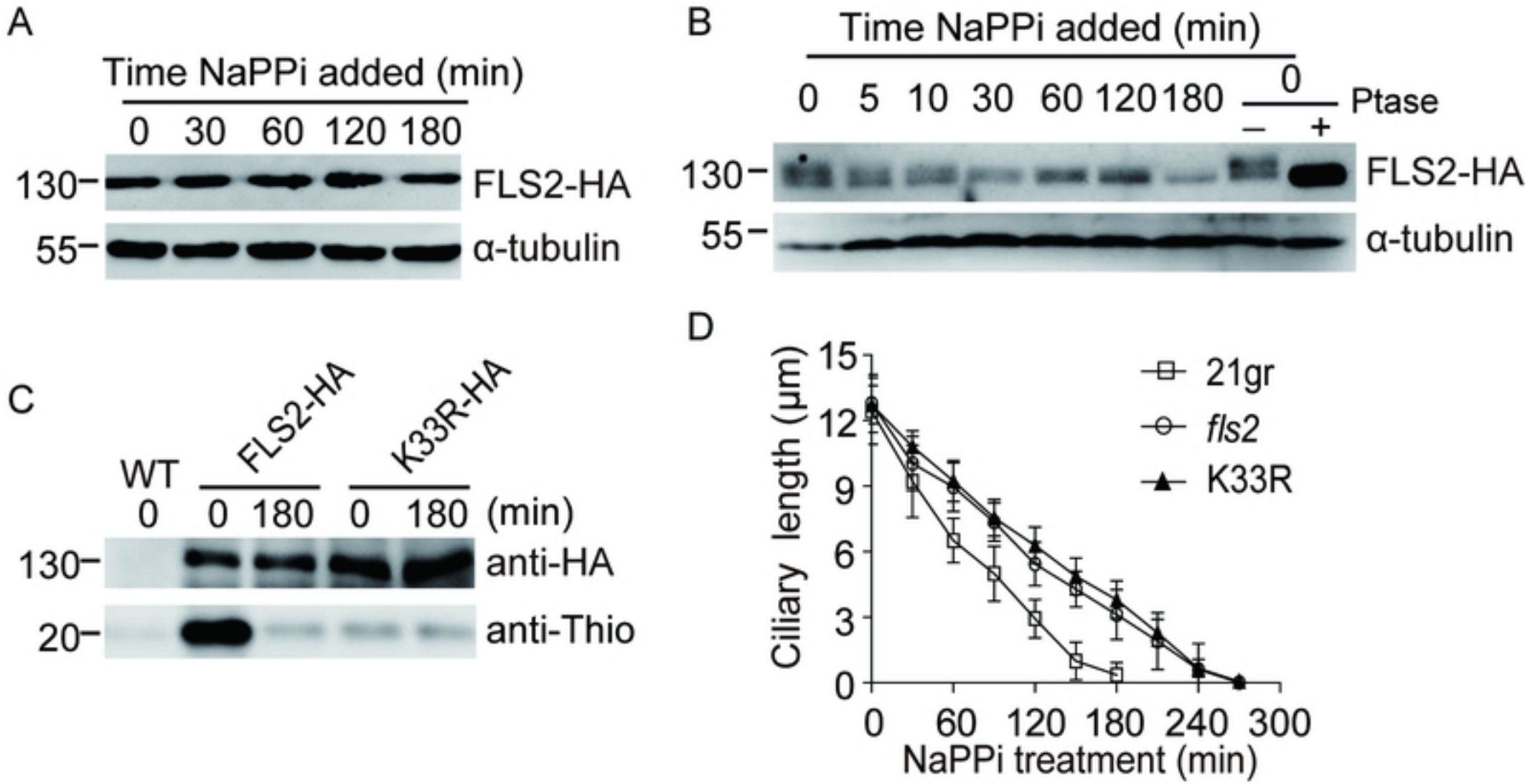

Figure3

Figure 4 Zhao et al.,

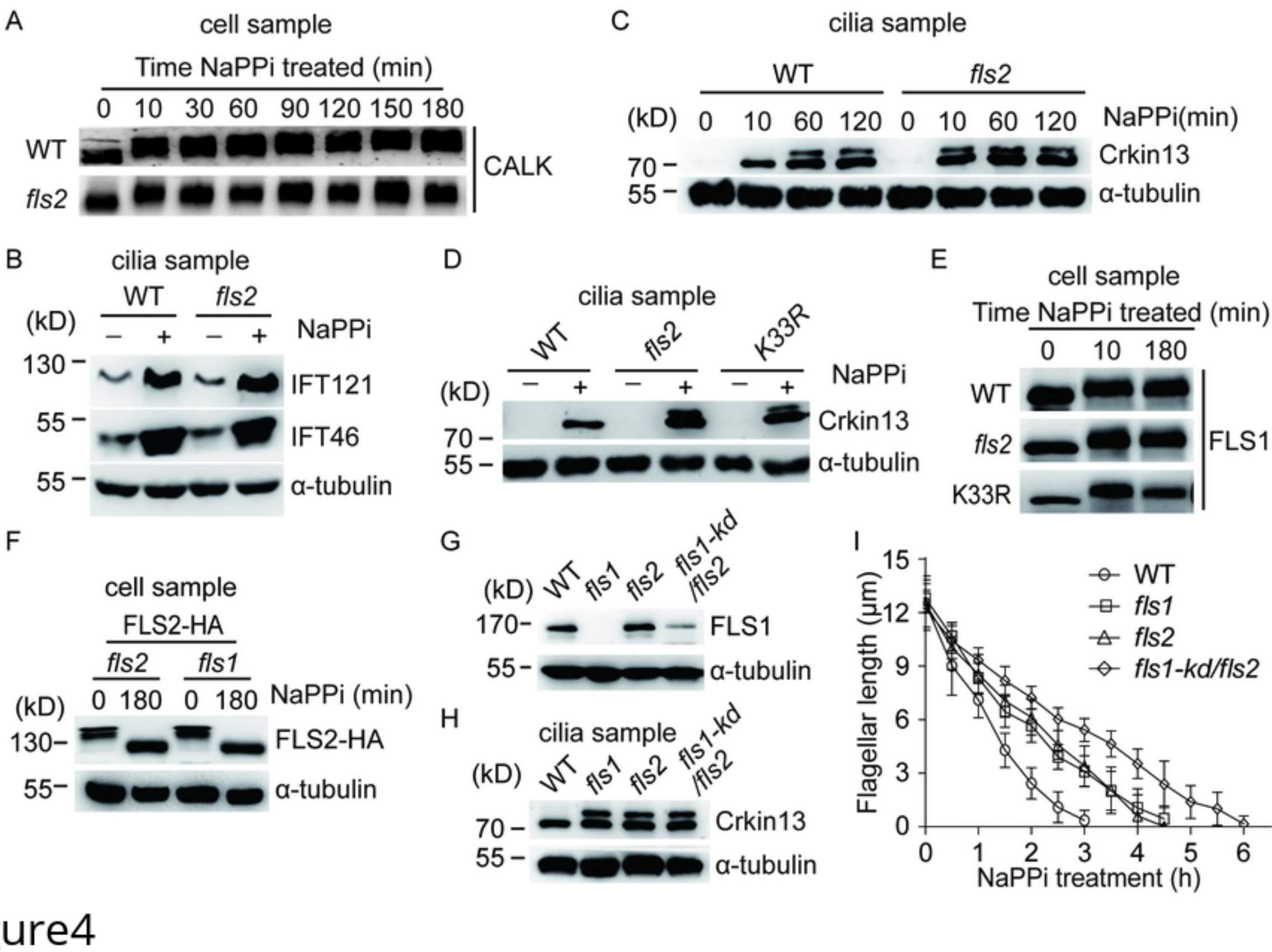

Figure4

Figure 5 Zhao et al.,

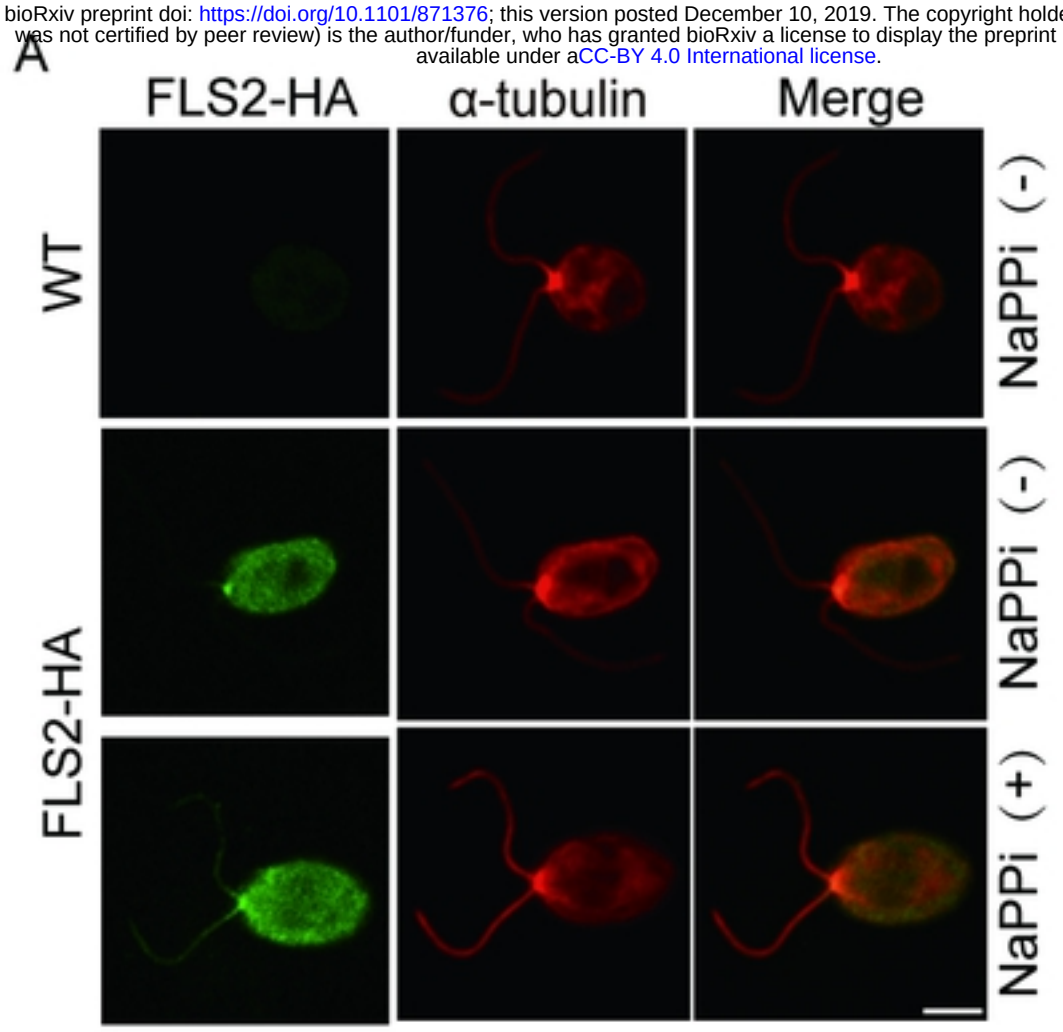

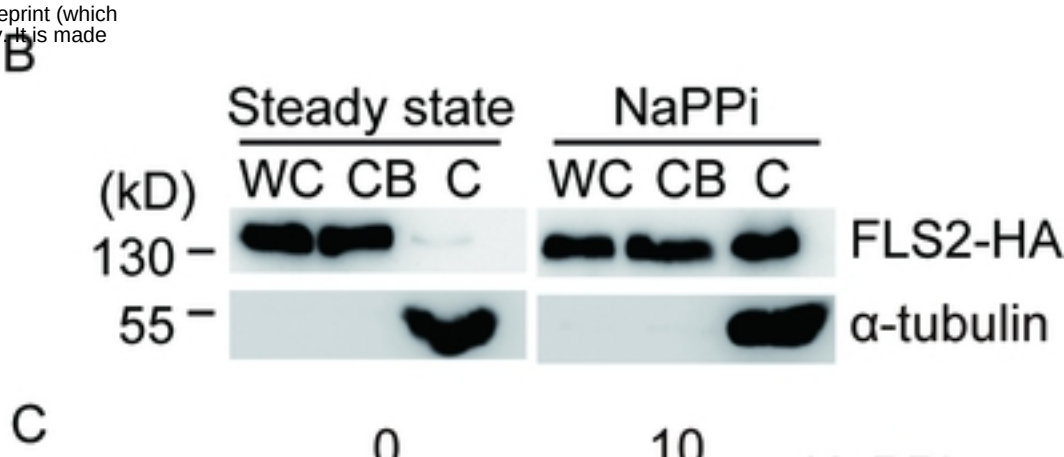

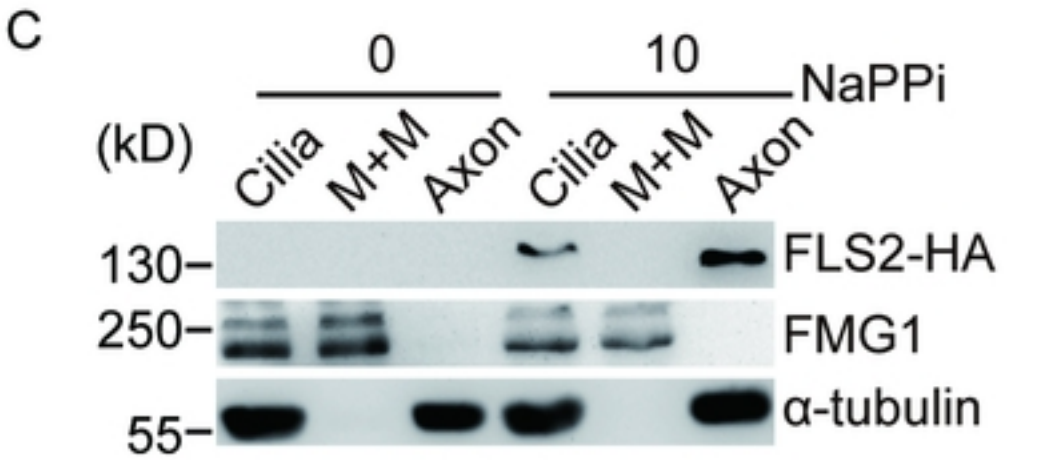

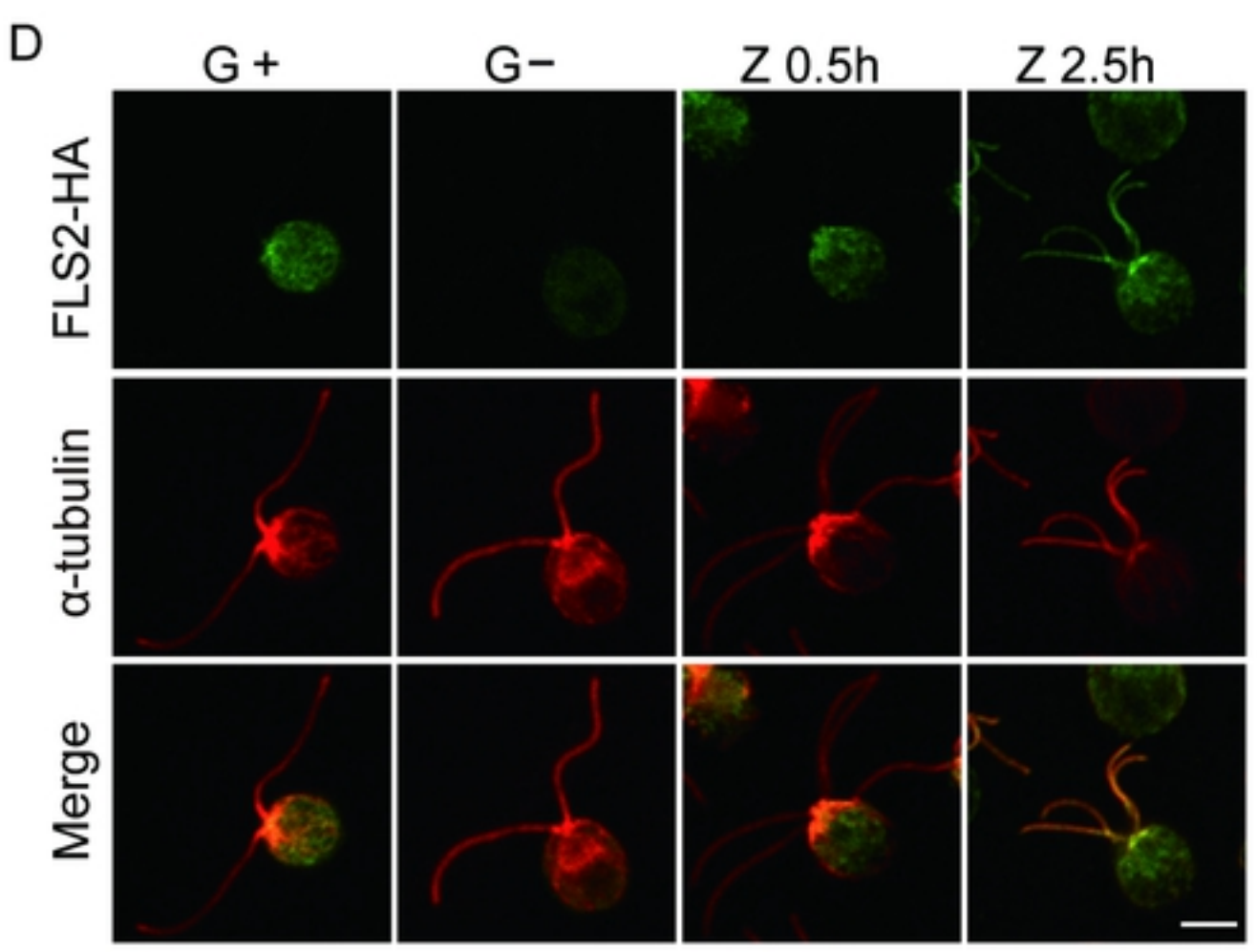

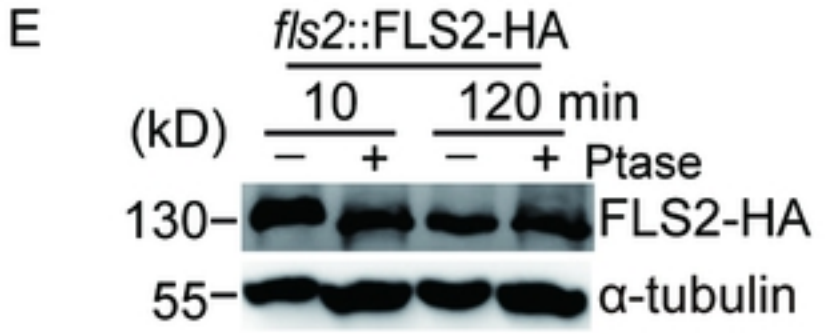

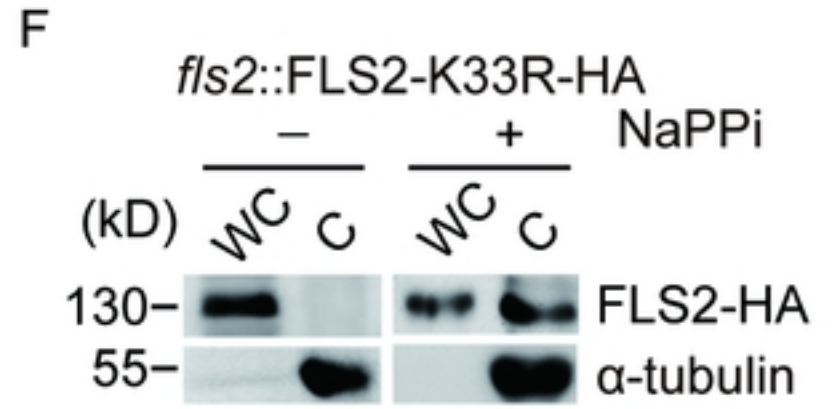

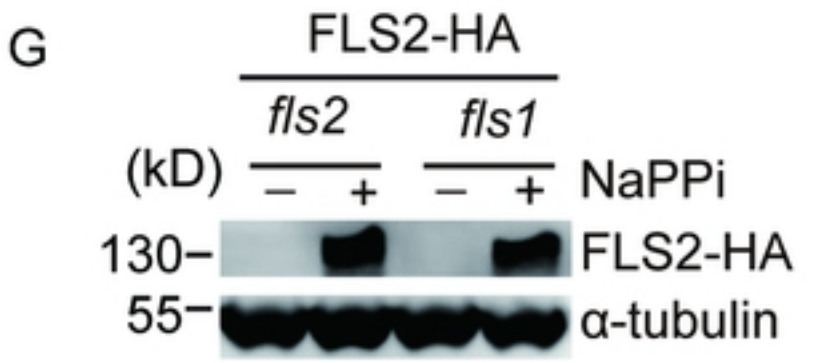

Figure5

Figure 6 Zhao et al.,

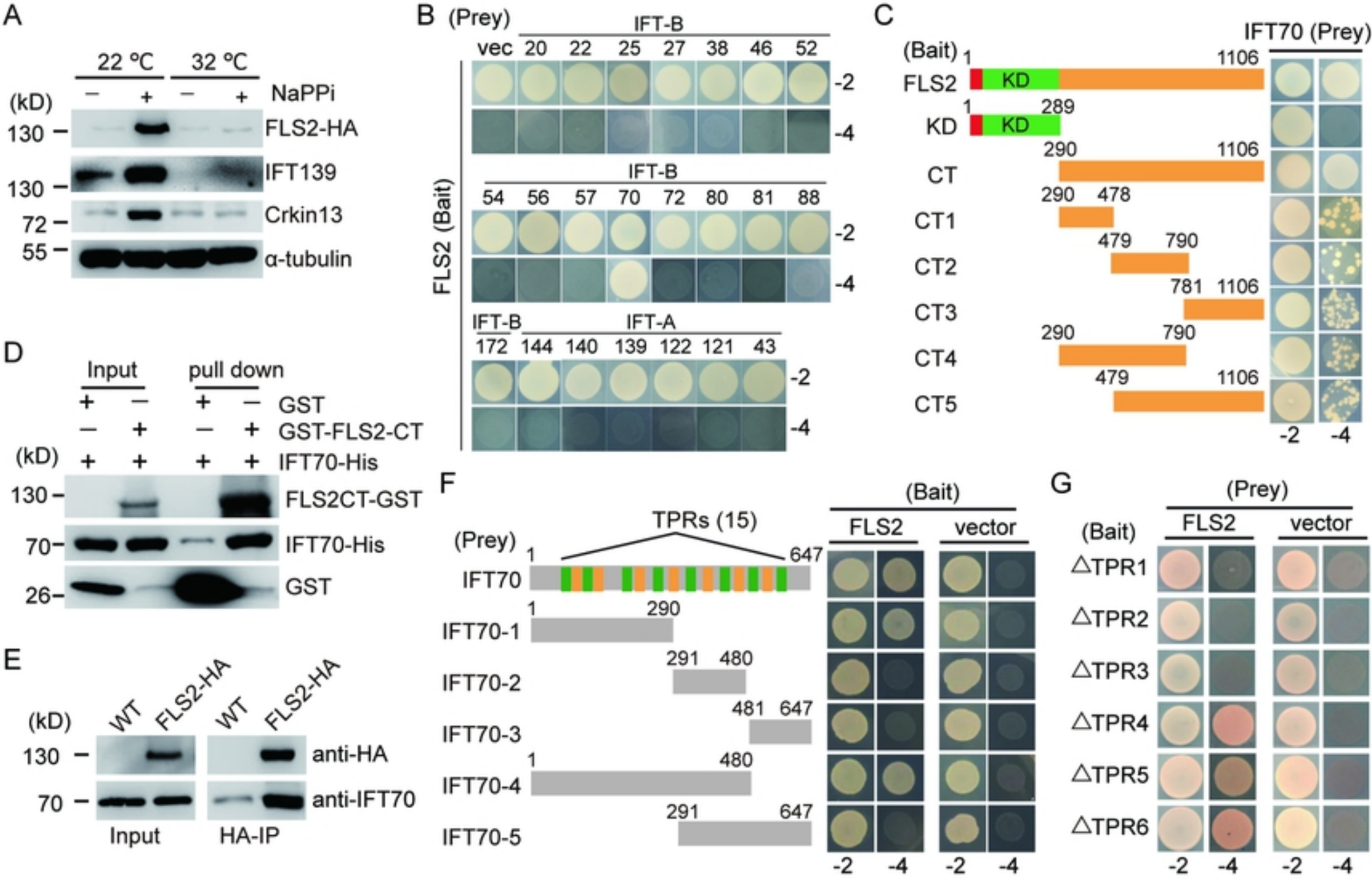

Figure6

Figure 7 Zhao et al.,

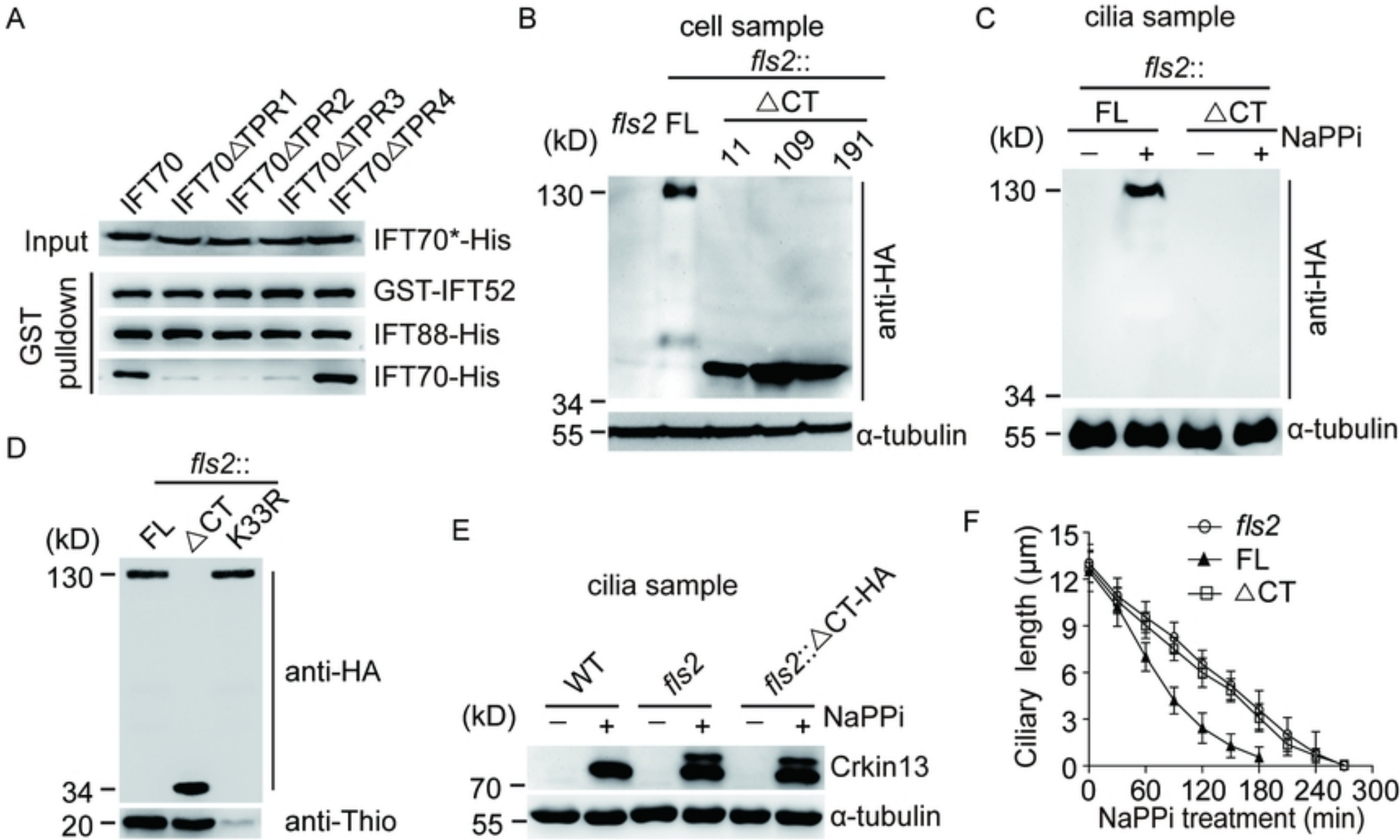

Figure7